Pedicel anatomy and histology in tomato vary according to genotype and water-deficit environment, affecting fruit mass

Jeanne Simon, Christelle Baptiste, Marc Lartaud, Jean-luc Verdeil, Béatrice Brunel, G. Vercambre, Michel Génard, Maïda Cardoso, Éric Alibert, Christophe Goze-Bac, et al.

Pedicel anatomy and histology in tomato vary according to genotype and water-deficit environment, affecting fruit mass

Jeanne Simon[a,b], Christelle Baptiste[d], Marc Lartaud[d], Jean-Luc Verdeil[d], Béatrice Brunel[a], Gilles Vercambre[a], Michel Génard[a], Maïda Cardoso[c], Eric Alibert[b], Christophe Goze-Bac[b], Nadia Bertin[a]*

[a]INRAE UR1115 Plantes et Systèmes de culture Horticoles - Site Agroparc - 84914, Avignon, France;
[b]Université Montpellier-CNRS, Laboratoire Charles Coulomb UMR 5221, F-34095, Montpellier, France;
[c]Université Montpellier, BNIF Imaging facility, F-34095, Montpellier, France;
[d]UMR AGAP, CIRAD, Montpellier, France

Email addresses: jeanne_simon@live.fr; christelle.baptiste@cirad.fr; jean-luc.verdeil@cirad.fr; beatrice.brunel@inrae.fr; gilles.vercambre@inrae.fr; michel.genard@inrae.fr; maida.cardoso@umontpellier.fr; eric.alibert@umontpellier.fr; christophe.goze@umontpellier.fr

* Corresponding author: Nadia Bertin (nadia.bertin@inrae.fr)

ABSTRACT

The growth and composition of fleshy fruits depend on resource acquisition and distribution in the plant. In tomato, the pedicel serves as the final connection between plant and fruit. However, very few quantitative data are available for the conducting tissues of the pedicel, nor is their genetic variability known. In the present study, a histological approach was combined with process-based modeling to evaluate the potential contribution made by the anatomy and histology of the pedicel to variations in fruit mass. Eleven genotypes were characterized and the impact of water deficit was studied for a single genotype using stress intensity and stage of application as variables. The results highlighted extensive variations in the relative proportions of the different pedicel tissues and in the absolute areas of xylem and phloem between genotypes. The model suggests that the variations in the area of the pedicel's vascular tissues

induced by differences in genotype and water-deficit environments partly contributed to fruit mass variability. They therefore warrant phenotyping for use in the development of plant strains adapted to future environmental constraints. The results also demonstrated the need to develop non-invasive *in vivo* measurement methods to establish the number and size of active vessels and the flow rates in these vessels to improve prediction of water fluxes in plant architecture.

KEYWORDS

Solanum lycopersicum, pedicel histology, water deficit, genotypic variability, virtual fruit model, xylem conductivity

1. INTRODUCTION

There is a pressing need to understand how we can adapt crops to the shifts in environmental constraints brought about by global change. For fleshy fruits, these constraints, in particular that of water availability, have a direct impact on yield and product quality because they affect the acquisition and distribution of resources in the plant. Water and minerals are transported from a plant's roots to its leaves and fruits mainly through the xylem vessels, while sugar and amino acids travel from the leaves to the sink organs through the sieve elements of the phloem [1]. Vascular tissues also transport molecules associated with the long-distance signaling system of the plant that play an important role in its response to stress [2,3]. Whereas the mechanisms involved in the regulation of water and carbon-assimilate distribution have been extensively studied, particularly in tomato (as one of the most-consumed fruit worldwide), the impact of the anatomical traits located in the conducting network has received less attention.

The vascular system undergoes intensive development during the early phase of flower-bud and fruit development and the hydraulic conductance of the truss peduncle and fruit pedicel increases as the tomato develops by means of secondary growth and the formation of new vessels, a process reflected in increased pedicel and peduncle diameters [4,5,6]. In the pedicel abscission zone (AZ), vessel differentiation and xylem lignification occur at a later stage, and the high hydraulic resistance at this point is

58 believed to result from the lower number of differentiated vessels, reducing the cross-sectional area of
59 the xylem relative to the rest of the pedicel [4,5,7]. This has been proposed as an explanation for the low
60 contribution made by the xylem to tomato fruit growth, since only 10-20% of the water entering the fruit
61 is carried by the xylem, while the remaining 80-90% is carried by the phloem [8,9,10,11]. However,
62 several studies have reported that more than 90 % of stem-to-fruit hydraulic resistance is located in the
63 tomato pericarp itself, and that the xylem tissues are functional and continuous throughout the pedicel,
64 including the AZ, remaining so throughout the development of the tomato fruit [12,13,14].

65 Resource availability and allocation to the fruit are greatly affected by non-optimal conditions. In the
66 case of xylem and phloem flows to the fruit, it has been shown that environmental impacts may be
67 mediated by changes in the water potential and osmotic gradients of the stem-pedicel-fruit continuum,
68 while the contributions made by vessel number and size have been described less fully. Several studies
69 show that xylem and phloem flows may be affected non-proportionally. For example, low light intensity
70 may decrease the total sap flow and increase the relative contribution of the xylem to the import of fruit
71 water [15]. Water deficit (WD) and high salinity can differentially affect sap influx through the phloem
72 and xylem tissues of the pedicel, and fruit water efflux via transpiration and xylem backflow [1,16,10].
73 The role of the AZ in preventing xylem backflow in periods of WD has been widely discussed [7,12,17].
74 Indeed, the hydraulic resistance of the pedicel AZ increases in plants grown under WD, in contrast to
75 the resistance levels observed on each side of the AZ, where new secondary vessels are formed [5]. In
76 line with this, WD reduces the pedicel xylem area, but increases the proportion of functional vessels on
77 either side of the AZ [18]. The impact of WD on fruit growth and composition is strongly dependent on
78 genotype and is exacerbated in large fruit genotypes [19]. Taking into consideration the genetic diversity
79 found in tomato responses to WD, a model-based study of the design of fruit ideotypes led to the hy-
80 pothesis that the conductance of the vascular tissues in the fruit pedicel could be of interest for the
81 adaptation of plants to WD [20]. The virtual fruit used in this study is a generic process-based model
82 that has been successfully applied to several species, including tomato [21,22]. This model simulates
83 the accumulation of water and dry matter during fruit growth, treating the fruit as a single large cell
84 connected to the stem by the pedicel vascular tissues and incorporates conductance values for each tis-

sue. Conductance is estimated using a relationship between xylem conductivity and the segment diameter of plant axes [23]. Despite the robustness of the model, this relationship, which was initially developed for peach trees, has never been tested using experimental data on herbaceous species such as tomato, which may limit its capacity to simulate fluxes under abiotic constraints [24]. Moreover, we lack data on the genetic diversity of pedicel anatomy although this has been shown to be a trait of interest in adapting plants to anticipated future water stress [20].

In the present study, we investigated genetic and WD-induced variability in cross-sectional areas of tomato pedicel tissues, particularly those of the xylem and phloem, by developing an image analysis pipeline. We observed eleven genotypes, both with and without AZs. We used the virtual fruit model to further explore the extent to which this variability observed at the pedicel level might contribute to variations in the fresh and dry mass of fruit. The value for tomato breeding of screening pedicel histological properties is discussed, as are the limitations of destructive and invasive approaches to the quantification of resistance along transport pathways, especially under WD.

2. MATERIAL AND METHODS

2.1 Plant material and growth conditions

The study investigated 11 contrasting tomato (*Solanum lycopersicum* L.) genotypes: West Virginia 106 (WVA106) a cherry tomato cultivar; the 8 parent genotypes of the MAGIC TOM population (Cervil, Criollo, Ferum, LA0147, LA1420, Levovil, PlovdivXXIVa (referred to here as Plovdiv); Stupicke Polni Rane (referred to here as Stupicke)) [25,19]; the wild type of the Heinz genotype; and a jointless mutant of Heinz with no AZ [26]. The Multi-parent Advanced Generation Inter-Cross population tomato (MAGIC TOM) population exhibits high allelic variability and includes small and large fruit genotypes from the *Solanum lycopersicum cerasiforme* group (Cervil, Criolo, Plovdiv, LA1420) and the *Solanum lycopersicum lycopersicum* group (LA0147, Ferum, Stupicke, Levovil) respectively. All plants were grown in a heated greenhouse (18 +/- 2 °C night / 22 +/- 4 °C day) in Avignon, in 5 L pots filled with humus (Klasmann, Substrat SP 15 %) and automatically watered with a commercial nutrient solution (Liquoplant Rose, Plantin, Courthézon, France) to match evaporative demand (control condition).

For the WD experiment, WVA106 plants were grown under three irrigation scenarios: the control scenario and two reduced-water scenarios (reductions of 50 % (mild WD), and 65 % (severe WD) compared to the control). For the severe WD scenario, the reduction was applied either 15 days before truss anthesis (early severe WD) or 4 days after truss anthesis (late severe WD). For the mild WD scenario, the reduction was applied 15 days before truss anthesis only (mild WD). Treatments were applied to single rows of 12 plants surrounded by border plants and each treatment was applied to two different rows (24 plants in total for each treatment). WD intensity was monitored in line with previous calibration experiments performed in the same greenhouse for the same genotype, with soil humidity targets of 1.6 (control), 1.0 (mild WD) and 0.6 (severe WD) $gH_2O\ g^{-1}$ of dried soil as described in Koch et al. [27]. The volume and frequency of irrigation increased as plants developed and varied daily depending on potential evapotranspiration (with a minimum of four daily irrigations). Soil relative humidity was monitored every other day using moisture content sensors (WCM-control, Grodan, Roermond, Netherlands) that had been previously calibrated by measuring soil aliquot humidity. Side-shoots were removed and trusses were pollinated with a vibrator three times a week. Fruit trusses were pruned to 10 set fruits per truss so that the fruit load was comparable in the control and WD scenarios. The greenhouse was whitewashed to avoid thermal stress.

2.2 Pedicel and fruit growth

The pedicel and the fruit diameters of the second proximal fruits (second from the stems) of trusses that developed concomitantly on all genotypes were measured with a caliper (Digimatic AOS 500-161-30) throughout development (from fruit set to maturity) on 4 to 8 plants of each genotype. The pedicel diameter was measured at three locations: the abscission zone itself (AZ); 5 to 10 mm from the AZ on the stem side (AZs); and 5 to 10 mm from the AZ on the fruit side (AZf) (Fig. 1A). At the red ripe stage of fruit ripening, pedicels were sampled and immediately fixed for histological analysis. The fruits were

weighed and dried in a ventilated oven to determine their fresh mass (FM), dry mass (DM) and dry matter content (DMC).

2.3 Histological pipeline to quantify the vascular tissue areas

A histological pipeline was developed to characterize the vascular elements in the truss peduncle, fruit pedicel and main stem collar (Fig. 1). First, fresh samples were fixed in Clarke's fixative solution (9 to 1 absolute ethanol to acetic acid by volume) to keep the tissue structure. Samples were then embedded in a 5 % agarose gel (Ref. LE-8200-B Sigma) and transversally cut using a vibratome (Microm HM 650 V). Slices were treated with a bleach solution (10 to 13 % available chlorine) to remove the cell content and increase contrast between tissues. Histological sections were stained overnight with a FASGA solution diluted at 1/7 [28], then rinsed in a 50 % glycerol solution. The FASGA mother solution was composed of 2 mL of safranin solution at 1 %, 14 mL of alcian blue solution at 0.5 %, 1 mL of acetic acid, 30 mL of glycerin and 19.5 mL of distilled water.

Glass slides were converted into high-resolution digital data with a Nanozoomer RS slide scanner (NanoZoomer Digital Pathology System, Hamamatsu, Japan). A plugin (PHIV_Tomate_toolset) was developed through Fiji [29] to measure the area of five anatomical zones corresponding to (from outer surface to center) the cortex, external phloem, secondary xylem, internal phloem and pith (Fig. 1C, D, E). Masks for the tissues were created semi-automatically using the plugin and then corrected manually (where necessary) before calculating the areas for each tissue. At least three slices from each pedicel were analyzed for each genotype and treatment.

Because the image resolution was not sufficient for quantitative analysis of the small vessels in the pedicel, the number and dimensions of xylem vessels located at the peduncle and main stem of WVA106 plants grown under control conditions were analyzed. Then, vessel diameter distributions were used to estimate a theoretical xylem conductivity, as described by the Hagen-Poiseuille equation [30]:

$$k_h = \left(\frac{\pi}{128\eta}\right) \sum_{i=1}^{n} \left(d_i^4\right) \quad (1)$$

where k_h is the theoretical conductivity of the xylem vessels ($m^4\ s^{-1}\ MPa^{-1}$), η is the dynamic viscosity of the sap (MPa s), d the diameter (m) of the ith vessel and n the number of vessels. We here assumed

the viscosity of the xylem sap to be equal to that of water (η = 10^{-9} MPa s at 20°C). These data were used to calibrate a relationship between segment diameter and xylem conductivity that was then extrapolated to the pedicel and applied in the modelling of the virtual fruit (see below).

2.4 Virtual fruit model and its calibration

A virtual fruit model was used to assess the potential impact of vascular tissues on fruit growth. This model predicts the changes in fruit water content over time resulting from the balance between xylem and phloem net influxes (including possible backflow), minus the water outflow due to fruit transpiration. The fruit is considered as a large single cell connected to the plant by the pedicel. Water is transported from the pedicel to the fruit's vascular system, which is composed of the fruit xylem and phloem, while sugars are transported from the pedicel phloem to the fruit phloem by mass flow. It is assumed that the phloem and xylem water potentials are the same and that local water exchanges can maintain this equilibrium [23]. The model also assumes that the quantities of water and sugars transported by the xylem and phloem are equal to the quantities of water and sugars that enter the fruit cells, i.e. it is assumed that water and sugars cannot be stored in the vessels [23]. In the pedicel, the phloem flow depends on pedicel phloem conductance (Lp1) and on the stem-to-fruit gradients of turgor pressure, while the xylem flow is driven by the difference in hydrostatic pressure between the stem and the fruit and depends on pedicel xylem conductance (Lx1) [23]. In the current version of the model, Lp1 and Lx1 are assumed to remain constant during fruit development. In the present study, Lx1 was estimated from the mean pedicel diameter for each genotype and treatment according to an experimentally adjusted power relationship between the stem and peduncle diameter and the xylem theoretical conductance calculated from the vessel diameter distribution using the Hagen-Poiseuille equation as described above (eq. 1; Fig. S1). Within the fruit, the xylem and phloem fluxes are calculated using non-equilibrium thermodynamic equations, which take into account the exchange surface area, which is assumed to be proportional to the fruit surface area. Other parameters are hydraulic conductivities, the solute reflection coefficient of the membrane separating the fruit from the vascular tissues, and hydrostatic and osmotic pressures calculated from the molar concentrations of osmotically active compounds (soluble sugars, organic acids, potassium…) [22].

Other than Lx1, model inputs are two measured climatic variables: air temperature and humidity; and two plant variables: stem water potential and the phloem sap concentration in sugars. The stem water potential varied daily from -2 bars to -4.6 bars for control irrigation, and from -2 bars to -6.5 bars and -8.0 bars respectively for mild and severe WD, based on experimental measurements taken before dawn and around noon from WVA106 using a pressure chamber (SAM Précis 2000 Gradignan, France). The phloem sap concentration was assumed to be constant and was taken from Liu et al [22].

The virtual fruit model was calibrated for each genotype. Eight parameters (Table 1), selected by sensitivity analysis and taken as genotypic parameters, were estimated in order to optimize simulation of the measured FM and DM during fruit development. All other parameters were taken from the literature and were similar for all genotypes [22,20]. In the case of the WD treatments applied to WVA106, a first estimation was performed which assumed that pedicel conductance alone was treatment dependent. A second simulation was then performed that included the effects of WD on both pedicel conductance and plant water status. The effect of WD on plant water status was accounted for by a decrease in stem water potential at noon from -4.6 bars for the control to -6.5 bars for mild WD and -8.0 bars for severe WD.

The eight estimated parameters relate to: (1) active uptake of sugars (nuM denotes maximal uptake rate, tstar and tauA determine, respectively, the time and rate of decrease in active uptake during fruit growth); (2) fruit plasticity (phiMax denotes maximal plasticity, k determines plasticity decrease with fruit age) and (3) conductivity and conductance (Lx and Lp denote, respectively, xylem and phloem conductivity in the fruit, and Lp1 denotes phloem conductance in the pedicel). The genetic algorithm NSGA-II [31] was used to obtain the combination of parameters that best predicts experimental dry and fresh weights from 10 daa (days after anthesis) to maturity for the small fruit genotype, and 16 daa to maturity for the large fruit genotype (ie from the end of the division period onwards). Outputs from this algorithm depend on the random initial values selected, so the optimization process was repeated 10 times.

The model's goodness of fit was evaluated through the Relative Root Mean Squared Error (RRMSE), a criterion commonly employed to quantify the mean difference between simulations and measurements:

$$RRMSE\ [\%] = \frac{100}{\overline{O_i}} \sqrt{\frac{\sum_{i=1}^{n}(O_i - S_i)^2}{n}} \qquad (2)$$

where O_i and S_i are, respectively, the observed and simulated values of fruit fresh and dry masses, and n is the number of observations.

2.6 Statistical analysis

All data were analyzed using R software [32]. Kruskal-Wallis and Tukey's range tests were used to compare the relative areas of vascular tissues, pedicel diameter, fruit fresh mass and dry matter content between genotypes and between the control and WD treatments. Statistical associations between the pedicel and fruit traits were assessed using the Kendal rank correlation coefficient. A Principal Component Analysis (PCA, "ade4" package developed for R software) was carried out on the parameter values estimated for each genotype, and the pedicel and fruit traits were projected as supplementary variables.

3. RESULTS

3.1 Histological quantification of vascular tissues along tomato pedicel

To assess the variability of conductive tissues around the abscission zone (AZ), the histological pipeline was first applied to the pedicels of two genotypes, Heinz wild type and Heinz Jointless, which differ in the presence (wild type) or absence (Jointless mutant) of an AZ. Average fruit differed significantly ($P<0.001$) between the two genotypes in terms of their final fruit fresh mass (FM was 73.1 g for the wild type and 52.4 g for the mutant) and dry matter content (DMC was 6.6 % for the wild type and 7.3 % for the mutant). No significant difference in the increase in pedicel diameter during fruit development between AZf and AZs was observed for any genotype (data not shown).

Histological properties at different locations along the pedicel were measured at fruit maturity (Fig. 2). At the AZ location in the wild type, the xylem tissues were clearly non-lignified and the area of each tissue could not be quantified (Fig. 2A). By contrast, in the mutant, a continuous lignification of the secondary xylem was observed at the location of the theoretical AZ (defined by pedicel curvature) (Fig. 2B). Comparing AZf and AZs, the proportion of secondary xylem to pedicel section was lower on the fruit side than on the stem side while the proportion of cortex was higher. This was observed both in the wild type (Fig. 2C) and the mutant (Fig. 2D), but these differences were significant for the wild type only ($P=0.013$). In the mutant, tissue proportions in the theoretical AZ were very close to those in the

AZs. For simplicity and given the lack of marked differences between AZs and AZf, in what follows, genotypic variability and environmental impact on tissue proportions were measured on AZf only.

3.2 Assessment of the genotypic variability of pedicel diameter and vascular tissue areas

Pedicel diameter and histology (AZf) were investigated in relation to fruit expansion in the two Heinz genotypes, in WVA106 (maturity only) and in the eight MAGIC TOM parent genotypes. In all genotypes, the increase in pedicel diameter during fruit development was observed to follow similar trajectories and ceased while the fruit was still rapidly expanding (Fig. 3). Observation of three classes of genotypes with significant differences in fresh mass ($P<0.01$; Fig. 4A) at fruit maturity (red ripe stage) showed that the smallest fruit had a significantly higher average DMC ($P<0.01$; Fig. 4B) and lower average pedicel diameter (Fig. 4C). The pedicel diameter correlated to the fruit FM (Kendal coefficient = 0.52; $P<0.0001$) and, to a lesser extent, to the fruit DMC (Kendal coefficient = -0.25; $P<0.002$). Histological analysis (see Fig. S2) showed that the cortex area was invariably the largest compared with other tissues in the pedicel section (33 to 67 % of the total section for all genotypes), followed by the secondary xylem (15 to 36 %) or by pith (10 to 30 %) depending on genotype. Meanwhile, the external (5 to 12 %) and internal (2 to 8 %) phloem areas were proportionally the lowest (Fig. 4D). In the vascular tissues, the proportion of the internal phloem was significantly lower in the small fruit class (4.5 %) compared to the medium and large fruit classes (5.9 %) ($P<0.01$). The proportions of the external phloem and secondary xylem were significantly higher in the medium fruit FM class (with averages of 8.9 % and 26.4 % respectively) compared to the two other classes (7.2 % and 21.6 % for the small fruit class and 7.3 % and 22.6 % for the large fruit class).

The mean absolute areas of the conducting tissues varied by a factor 4 to 6 among genotypes. The secondary xylem was always the largest and the internal phloem always the smallest (Fig. 4E). On average, areas in the small fruit class were 3 times less for the internal phloem, 2 times less for the external phloem and 2 times less for the secondary xylem compared with the two other fruit classes ($P<0.001$). The ratio of internal phloem to external phloem was 0.64, 0.67, and 0.82 in the small, medium and large fruit classes respectively, with a significant difference between the two extremes ($P=0.03$). The total phloem (internal + external) to xylem ratio was, on average, 0.53, 0.58, 0.60 for the small, medium and

large fruit respectively, but these differences were not significant. Figure S2 depicts the genotypic variability in pedicel histology and suggests that not only were the proportion and areas of the tissues affected, but also the size and density of the vessels of the xylem tissue. These data have the potential to be highly important, but unfortunately, at this image resolution, it was not possible to distinguish between small vessels, tracheids and parenchyma rays.

3.3 Impact of water deficit on pedicel diameter and on the vascular tissues of the tomato pedicel in relation to fruit growth

The anatomy of the pedicel was observed under three WD scenarios applied to genotype WVA106. All of them significantly reduced fruit FM compared to the control (-13 %, -24 % and -27 %, for mild WD, early severe WD and late severe WD respectively), and significantly increased DMC (+24 %, +24 % and +16 %, for mild WD, early severe WD and late severe WD respectively) (Figs. 5A, 5B). Fruit DM was significantly reduced only in the late severe WD scenario (-15 % compared to the control) and was unchanged in the early deficit treatments.

Early severe WD provoked a significant reduction in pedicel diameter (-25 %; Fig. 5C), which translated into a significant reduction in the absolute areas of the secondary xylem (-54 %), pith (-63 %), external phloem (-55 %) and internal phloem (-51 %), whereas cortex area was affected only slightly (Fig. 5D). This led to a significant decrease in the proportions of the secondary xylem (-18.6 %) and the pith (-33.3 %), and a significant increase in cortex proportion (+21.3 %), while the proportions of the phloem tissues were not affected (Fig. 5E). The mild WD treatment did not affect pedicel diameter, but it provoked a significant reduction in pith absolute area compared with the control (-53 %), also changing the tissue proportions in the pedicel section: cortex proportion increased (+12.8 %), while pith (-39.4 %) and internal phloem (-16.6 %) proportions decreased. Late severe WD did not significantly affect pedicel diameter or tissue areas; these were probably already fixed by the time of the WD treatment and correspond to the kinetics shown in Fig. 3A. The ratio of internal to external phloem areas was stable showing no significant effects from the treatments (mean of 0.75; $P = 0.77$), as was the total phloem to xylem ratio (mean of 0.58; $P = 0.59$).

3.4 Model-based analysis of the potential contribution made by pedicel anatomy to genetic and WD-induced variability in tomato fruit mass

The virtual fruit model described above was used to analyse the contribution of pedicel growth to genotypic and WD-induced effects on fruit fresh and dry masses. The xylem conductance of the pedicel (Lx1) was estimated on the basis of final pedicel diameter (mean value for each genotype and treatment) as described in Materials and Methods (Fig. S1). Because the pedicel diameter plateaued from the beginning of the simulation (initiated after cell division was complete) a constant value was applied. Assuming a pedicel length of 2 cm, the estimated values of Lx1 ranged from 1.6 x 10^{-8} m^3 MPa^{-1} s^{-1} for WVA106, to 2.4 x 10^{-7} m^3 MPa^{-1} s^{-1} for the Ferum genotype under the control irrigation regime. Values went down to 4.5 x 10^{-9} m^3 MPa^{-1} s^{-1} under the early severe WD treatment but were barely affected under the other two WD treatments. Estimated values of the eight genotype-dependent parameters are given in Table S1.

The model showed a fairly good fit for the genotypic variations in fruit mass under the control irrigation regime, with an average RRMSE of 6.4 % for FM and 8.3 % for DM (Fig. S3). In the WD scenarios, when the impact of WD on pedicel conductance (Lx1) alone was considered, the decrease in fruit fresh mass under WD was poorly predicted (RRMSE was 32 % and 20 % for FM and DM respectively, under mild WD; 51 % and 9 % for FM and DM under early severe WD; and 58 % and 1.3 % for FM and DM under late severe WD) (data not shown). The accuracy of FM predictions showed general improvement (RRMSE was 20 % for mild WD and 30 % on average for the two severe WD scenarios) when the combined effects of WD on both Lx1 and plant water status were included (Fig. S3A). These simulations suggest that, where WD is concerned, the primary constraint on the entry of water into the fruit is the plant water status rather than a decrease in pedicel conductivity. By contrast, fruit DM did not depend on Lx1 or stem water potential and was underestimated by the model except in the early severe WD scenario (Fig. S3B). These results are in fair agreement with experimental data, where early WD treatments were shown to have no significant impact on fruit DM.

A PCA was performed on the values for the eight parameters estimated for each genotype (Table 1), to which projections of the pedicel and fruit traits were added as supplementary variables (Fig. 6). The first two dimensions accounted for 56.4 % of the total variance. Parameter tauA, involved in both active

sugar uptake and the xylem conductivity of the fruit (Lx) and pedicel (Lx1), positively contributed to the first component, while parameter k, involved in cell expansion, negatively contributed to this component. The second dimension mainly showed opposing values for phloem conductivity in the fruit (Lp) compared with that in the pedicel (Lp1), and between two parameters involved in active sugar uptake (nuM and tstar). Other parameters and traits, such as maximum cell wall extensibility and the phloem to xylem ratio did not generate differences. The three classes of fruit FM were clearly separated on this plane; small and large fruit were differentiated in the first component and medium fruit in the second component. Projections of fruit and pedicel traits on this plane suggest that large fruit FM was associated with large absolute areas of the xylem (secxyl_absval) and phloem (extphl_absval and intphl_absval) in the pedicel, high xylem conductivity in the fruit and pedicel, and a slower decrease in active sugar uptake during fruit ageing (tauA). Conversely, small fruit with high DMC were associated with a higher maximum active sugar uptake (nuM) and an earlier decrease in cell plasticity during fruit aging (k), which could be indirectly related to a shorter expansion phase in small-fruit genotypes compared with large-fruit genotypes. Within these two classes, WVA106 and Ferum showed a contrasting distribution along the second component compared with the other genotypes of their respectively class. These genotypes, along with the genotypes from the medium fruit FM class, were associated with high values for the external phloem and secondary xylem relative areas (extphl_relval, intphl_relval and secxyl_relval), phloem conductance in the pedicel (Lp1), and a decrease in maximum active sugar uptake (tstar) in the course of fruit development, but exhibited low values for phloem conductivity in the fruit (Lp) and maximum active sugar uptake (nuM).

4. DISCUSSION

Xylem and phloem flows depend on pressure gradients in the whole plant system and on the anatomical and hydraulic properties of the network [33]. Vascular tissue has been shown to have both deterministic and plastic properties and could act as a primary driving force for plant diversification and adaptation to particular growth conditions [34]. The pedicel is the final structure connecting the fruit to the plant. In the present study, by coupling a histological approach with modeling, we showed that there is a wide

genetic variability in the pedicel vasculature, that has rarely been described for tomato or, more generally, for herbaceous plants, and we confirmed the interest of this trait for the selection of tomato cultivars adapted to water deficit conditions.

4.1 The decrease in the vascular tissue area of the pedicel is not dependent on the presence of an abscission zone

Many studies have focused on hydraulic resistance in the tomato pedicel and the impact of this on the supply of water and minerals (calcium in particular) to the fruit [35,12,5,6]. In the present study, a clear discontinuity in xylem lignification was observed at the abscission point, agreeing with the findings of a previous study on tomato [36], together with a decrease in the xylem proportion along the pedicel, which was independent of the presence or absence of an AZ. Pedicel sections and xylem and phloem tissue areas were very similar between the Jointless mutant and the wild type. However, despite the absence of an AZ, the Jointless mutant had a smaller fruit FM and a higher DMC. This is counter-intuitive since the hydraulic resistance along the pedicel should be lower for the mutant than for the wild type [5]. When taken together, these results suggest that the increasing hydraulic resistance along the pedicel mainly results from the decrease in area of the conductive tissues, in agreement with previous studies [4,7,6], rather than from a local disruption. They also support the hypothesis that the non-lignification of xylem tissues in the AZ does not necessarily reduce the overall hydraulic conductivity to a significant degree, meaning that only the mechanical components of the xylem (the fibres and xylem parenchyma) are constricted [12] or that the role of xylem conductance is minor compared with phloem flow, as is suggested by the literature on water transport in tomato fruit [8]. However, this second hypothesis is brought into question by the strong association observed between fruit mass and xylem conductance in the pedicel, which was associated with a large absolute area of xylem tissue (Fig. 6). Having applied MRI at the truss peduncle level, Windt et al. [13] suggested that the contribution of the xylem to the import of water in tomato could be much greater than that commonly recorded using destructive methods. It may therefore be necessary for further experimental studies to revisit the relative contribution of the xylem and the phloem to water supply in tomato by integrating xylem backflow and xylem-phloem exchanges within the pedicel.

4.2 Pedicel anatomical traits warrant phenotyping for the screening of genetic resources

Constantinescu et al. [20] suggested that pedicel conductivity and active uptake of sugars could be traits of interest for tomato breeding as routes to maintain the fresh mass of large-fruit genotypes under WD and to increase their dry matter content under well-irrigated conditions. The present study revealed a high variability according to genotype in the absolute areas of the xylem and phloem that has never been previously reported. As expected, the largest fruit also have the largest pedicel sections overall. However, our data reveal variations in the different tissues. The internal phloem appeared to be the most variable tissue in the pedicel for the genotypes investigated. In tomato, fruit trusses are mainly supplied by the two leaves located below the truss through the upward movement of assimilates in the internal phloem [37], which is in line with the positive correlation observed between internal phloem area and FM (Fig. 6). However, FM was also associated with the absolute areas of the xylem and external phloem since in large fruit genotypes all vascular tissues increased more or less proportionally to the pedicel diameter. This agrees with reported lower levels of xylem production in the AZs of pedicels from mature cherry tomatoes compared to those in large-fruit cultivars [4]. Interestingly, the internal to external phloem ratio increased from small to large fruit genotypes, but the ratio between phloem and xylem areas remained relatively constant, at around 57 %. Additional genotypes should be investigated to confirm these results and it would be an easy matter to use the analysis pipeline developed in this study for further exploration of the genetic diversity found in pedicel histology.

Without doubt, such variations in the area and proportion of tissues have an effect on water and carbon fluxes and therefore cannot be ignored in predictive models of fruit growth. In the virtual fruit model initially developed for peach trees, the xylem conductivity of the plant axis (stem, truss peduncle or fruit pedicel) is related to the segment diameter and this relationship was newly calibrated in the present study for tomato (Fig. S1). The values for xylem conductivity in the pedicel, estimated on the basis of the pedicel diameter, ranged from 3.1 x 10^{-10} m^4 MPa^{-1} s^{-1} for cherry tomato (WVA106) to 4.9 x 10^{-9} m^4 MPa^{-1} s^{-1} for large fruit genotypes (Ferum). These values lie within the range reported in the literature for other species. In mango, pedicel conductivity values between 2.2 x 10^{-10} and 8.4 x 10^{-9} m^4 MPa^{-1} s^{-1} were measured using the flow meter method [38]. In cherry tomato, the conductivity of the functional

xylem, measured in the pedicel sections as the percentage of dye-stained bundles, was estimated to range from 4.3 x 10^{-9} m^4 MPa^{-1} s^{-1} in AZf to 3.0 x 10^{-7} m^4 MPa^{-1} s^{-1} in AZs [18]. Conductance values estimated using the suction method for the tomato pedicel range from 11 x 10^{-10} to 5.5 x 10^{-9} m^3 MPa^{-1} s^{-1}, depending on developmental stage and genotype [5,14]. Interestingly, in a detached cherry pedicel, conductance measured using pressure-volume curves was about three- to fourfold lower than predicted from the numbers and diameters of the xylem vessels [39].

Investigation at vessel scale is likely to provide more precise information, given the variability of vessel densities in the tissue (see Fig. S2). Experiments should not be confined to the investigation of the number and size of dye-stained vessels in excised organs, but should also examine the number of active vessels over time in the living plant, for instance through the use of MRI measurements [40,41,42]. When no such data is available, the pedicel diameter appears to be a valuable proxy for modeling.

4.3 The effect of water deficit on pedicel histology only partly explains its effects on fruit mass and dry matter content

Although many factors, such as stem water potential, sap sugar concentration and viscosity, osmotic accumulation, etc., are involved in the fruit water balance under WD [8,19,43,44], the present study was designed to assess the specific contribution of the pedicel anatomy *per se*. The early WD treatments affected the whole period of fruit development including cell division, while the late WD treatment impacted mostly on the cell expansion period. Indeed, in WVA106, cell division ends at about 10 daa, corresponding to the first third of the development period [45]. Assuming that the increase in pedicel diameter reflects the production of new vessels during secondary growth [5], then, according to Fig. 3, the number of vessels was fixed before fruit cell division ceased. This is confirmed by the reduction of both pedicel diameter and vascular tissue areas under the early severe WD scenario, but not under late severe WD. The reduction of the xylem area is not sufficient to state that the conductive vessel area has been reduced, because it is possible that the proportion of non-conductive xylem tissue has also varied [14]. However, several studies have shown that WD decreases the diameter of xylem vessels in tomato pedicel [18], grape [46] and maize [47]. Under severe WD, Lx1 estimated from pedicel diameter de-

creased by 71 % compared to the control (Table S1). Despite this substantial reduction, the model simulations showed that it is mainly the inclusion of the water status of the plant, *via* the reduction of the stem water potential that provides a good fit for the reduction in the fruit's final fresh mass. It is thus the water status of the plant rather than the xylem conductance of the pedicel that controls the supply of water to the fruit under WD, in accordance with the results of Li et al. [14] obtained on detached fruit deprived of phloem flow using a jointless tomato genotype. It also confirms that the greatest resistance to water transport occurs in the fruit itself rather than in the pedicel, as reported for tomato [12] and kiwi fruit [48]. Supporting this, the estimated fruit conductivity in our study was more than 1000 times lower than pedicel conductivity (Table S1). Thus, a better understanding and improved description of the architecture of the vascular tissues and their properties within the fruit will be a major requirement for the modeling of fruit growth and quality, as has previously been illustrated through X-ray micro-tomography [48] and modeling [24].

The phloem also undoubtedly plays a role in the fruit water balance under WD conditions. In our study, the severe stress treatment affected the internal and external xylem and phloem areas proportionally (-53 % on average) while tissue ratios remained generally stable. It may be hypothesized that all conductivity pathways were affected proportionally. However, fruit dry weight was not affected by early WD, suggesting either that no marked reduction occurred in phloem flow or that phloem sap concentration increased [16]. These effects are difficult to quantify and model mechanistically due to the multiple factors involved other than tissue surface. Modeling of water flow through the pedicel and into the fruit has suggested that water import into the young growing tomato may be limited primarily by phloem conductivity in the pedicel, related to the size of the sieve tube elements and sap viscosity [43,50]. Another study used the virtual fruit model to suggest that bi-directional exchanges of water between phloem and xylem may regulate diurnal and nocturnal sugar flows to the fruit and buffer the variations of sugars in the pedicel, while xylem-to-apoplast recirculation of water through the fruit phloem may reduce xylem backflow at midday [51].

Additionally, although changes in tissue area are proportional, the relative contributions of the phloem and xylem tissue to water import may vary in response to WD. Indeed, a strong environmental effect on the relative contribution of the xylem to tomato fruit growth has been reported in different studies (e.g.

[15] for light; [16] for salinity). These variations may result from environmental effects on the constituent number and size of xylem vessels determined during fruit development, but also from short-term reversible variations in the number of active vessels, *i.e*. when these are mobilized to transport water around the plant architecture in response to fluctuations in environmental conditions. As a consequence, there will be a need to carry out *in vivo* investigation and modelling of the number and diameter distribution of the conducting elements that are functional at any given time.

4.4 Concluding remarks and perspectives

The present study has identified, for the first time, a high genetic variability in pedicel histology, i.e. xylem and phloem areas, which contributes to the genetic variability of fruit mass. This could be a trait of interest for the phenotyping of plants that are better adapted to WD. For modeling purposes, pedicel diameter provides a simple measurable proxy for the estimation of xylem conductivity, but major challenges are presented by the need to investigate hydraulic properties at vessel scale and *in vivo* under fluctuating environmental conditions if we are to improve understanding and modeling of the phloem and xylem flows to the fruit.

Acknowledgements

We thank Guillaume Garcia, Thibault Crouzet and Pierre Valsesia for their valuable contributions to this work.

Availability of data and materials

All relevant data are available in the paper and Supplementary Files.

Funding

This work was funded by the «Investissements d'avenir» (Labex Agro:ANR-10-LABX-0001-01) program, within the I-SITE MUSE (ANR-16-IDEX-0006) framework, and by INRAE's AgroEcoSystem division.

Author contributions

M. C., B. B., E. A., C. B. and J. S. carried out the experiments. C. G.-B., N. B. and J. S. designed the project. M. C., M. L., G. V., M. G., J.-L. V. and J. S. contributed to data analysis. N. B., C. G.-B. and J. S. wrote the manuscript. M.G., M. C., G. V. and J.-L. V. proofread the manuscript.

Declaration of Competing Interests

The authors declare that there is no conflict of interests.

References

[1] L.C. Ho, The mechanism of assimilate partitioning and carbohydrate compartmentation in fruit in relation to the quality and yield of tomato, J. of Exp. Bot. 47 (1996) 1239-1243.

[2] T.J Lough, W.J. Lucas, Integrative plant biology: role of phloem long-distance macromolecular trafficking, Annual Reviews of Plant Biology 57 (2006) 203-232.

[3] Z. Spiegelman, B.K. Ham, Z. Zhang, T.W. Toal, S.M. Brady, Y. Zheng, Z. Fei, W.J. Lucas, S. Wolf, A tomato phloem-mobile protein regulates the shoot-to-root ratio by mediating the auxin response in distant organs, The Plant Journal 83 (2015) 853-863.

[4] J.P. André, A.M. Catesson,, M. Liberman, Characters and origin of vessels with heterogenous structure in leaf and flower abscission zones, Canadian Journal of Botany 77 (1999) 253-261.

[5] W. Van Ieperen, V.S. Volkov, U. Van Meeteren, Distribution of xylem hydraulic resistance in fruiting truss of tomato influenced by water stress, Journal of Experimental Botany 54 (2003) 317-324.

514 [6] D. Rančić, S.P Quarrie, I. Pećinar, Anatomy of tomato fruit and fruit pedicel during fruit development, Mi-
515 croscopy: Science, Technology, Applications and Education 2 (2010) 851-861.
516 [7] D.R. Lee, Vasculature of the abscission zone of tomato fruit: implications for transport, Canadian Journal of
517 Botany 67 (1989) 1898-1902.
518 [8] L.C. Ho, R.I. Grange, A.J. Picken, An analysis of the accumulation of water and dry matter in tomato fruit,
519 Plant Cell Environment 10 (1987) 157-162.
520 [9] A.J.E. Van Bel, Xylem-phloem exchange via the rays: the undervalued route of transport, Journal of Experi-
521 mental Botany 41 (1990) 631-644.
522 [10] S. Guichard, C. Gary, C. Leonardi, N. Bertin, Analysis of growth and water relations of tomato fruit in
523 relation to air vapor pressure deficit and plant fruit load, Journal of Plant Growth Regulation 24 (2005) 201.
524 [11] B.A.E. Van de Wal, W. Carel, C.W. Windt, O. Leroux, K. Steppe, Heat girdling does not affect xylem
525 integrity: an in vivo magnetic resonance imaging study in the tomato peduncle, New Phytologist 2015 (2017)
526 558-68.
527 [12] M. Malone, J. Andrews, The distribution of xylem hydraulic resistance in the fruiting truss of tomato,
528 Plant Cell Environment 24 (2001) 565-570.
529 [13] C.W. Windt, E.Gerkema, H.Van As, Most water in the tomato truss is imported through the xylem, not
530 the phloem: a nuclear magnetic resonance flow imaging study, Plant Physiology 151 (2009) 830-842.
531 [14] H. Li, X. Zhang, X. Hou, T. Du, Developmental and water deficit-induced changes in hydraulic proper-
532 ties and xylem anatomy of tomato fruit and pedicels, Journal of Experimental Botany 72 (2021) 2741–2756.
533 [15] J. Hanssens, T. De Swaef, K.Steppe, High light decreases xylem contribution to fruit growth in tomato.
534 Plant Cell Environment 38 (2015) 487-498.
535 [16] Z. Plaut, A. Grava, C. Yehezkel, E. Matan, How do salinity and water stress affect transport of water,
536 assimilates and ions to tomato fruits? Physiologia Plantarum 122 (2004) 422-442.
537 [17] S. Guichard, N. Bertin, C. Leonardi, C. Gary, Tomato fruit quality in relation to water and carbon fluxes,
538 Agronomie 21 (2001) 385-392.
539 [18] D. Rančić, S.P. Quarrie, M. Terzić, S. Savić, R. Stikić, Comparison of light and fluorescence micros-
540 copy for xylem analysis in tomato pedicels during fruit development, Journal of microscopy 232 (2008) 618-
541 622.

[19] J. Ripoll, L. Urban, N. Bertin, The potential of the MAGIC TOM parental accessions to explore the genetic variability in tomato acclimation to repeated cycles of water deficit and recovery, Frontiers in plant science 6 (2016) 1172.

[20] D. Constantinescu, M.M. Memmah, G. Vercambre, M. Génard, V. Baldazzi, M. Causse, E. Albert, B. Brunel, P. Valsesia, N. Bertin, Model-assisted estimation of the genetic variability in physiological parameters related to tomato fruit growth under contrasted water conditions, Frontiers in plant science 7 (2016) 1841.

[21] S. Fishman, M. Génard, A biophysical model of fruit growth: simulation of seasonal and diurnal dynamics of mass, Plant Cell Environment 21 (1998) 739–752.

[22] H. F. Liu, M. Génard, S. Guichard, N. Bertin, Model-assisted analysis of tomato fruit growth in relation to carbon and water fluxes, Journal of Experimental Botany 58 (2007) 3567-3580.

[23] A.J. Hall, P.E.H. Minchin, M.J. Clearwater, M. Génard, A biophysical model of kiwifruit (Actinidia deliciosa) berry development, Journal of Experimental Botany 64 (2013) 5473–5483.

[24] M. Cieslak, M. Génard, F. Boudon, V. Baldazzi, C. Godin, N. Bertin, Integrating physiological and architectural perspectives in models of fruit development facilitates detailed studies of their impact on fruit quality, Front. Plant Sci. 7 (2016) 1739.

[25] L. Pascual, N. Desplat, B.E. Huang, A. Desgroux, L. Bruguier, J.P. Bouchet, G.H. Le, B. Chauchard, P. Verschave, M. Causse, Potential of a tomato MAGIC population to decipher the genetic control of quantitative traits and detect causal variants in the resequencing era, Plant biotechnology journal 13 (2015) 565-577.

[26] L. Mao, D. Begum, H.W. Chuang, M.A. Budiman, E.J. Szymkowiak, E.E. Irish, R.A. Wing, JOINTLESS is a MADS-box gene controlling tomato flower abscission zone development, Nature 406 (2000) 910-913.

[27] G. Koch, G. Rolland, M. Dauzat, A. Bédiée, V. Baldazzi, N. Bertin, Y. Guédon, C. Granier, Leaf Production and Expansion: A Generalized Response to Drought Stresses from Cells to Whole Leaf Biomass—A Case Study in the Tomato Compound Leaf, Plants 8 (2019) 409.

[28] D. Tolivia, J. Tolivia, Fasga: a new polychromatic method for simultaneous and differential staining of plant tissues, Journal of Microscopy 148 (1987) 113-117.

[29] J. Schindelin, I. Arganda-Carreras, E. Frise, V. Kaynig, M. Longair, T. Pietzsch, S. Preibisch, C. Rueden, S. Saalfeld, B. Schmid, J-Y. Tinevez, D.J. White, V. Hartenstein, K. Eliceiri, P. Tomancak, A. Cardona, Fiji: an open-source platform for biological-image analysis, Nature methods 9 (2012) 676-682.

[30] H.W. Calkin, A.C. Gibson, P.S. Nobel, Xylem water potentials and hydraulic conductances in eight species of ferns, Canadian Journal of Botany 63 (1985) 632-637.

[31] K. Deb, A. Pratap, S. Agarwal, T.A.M.T. Meyarivan, A fast and elitist multiobjective genetic algorithm: NSGA-II, EEE transactions on evolutionary computation 6 (2002) 182–197.

[32] R Core Team, R: A language and environment for statistical computing, R Foundation for Statistical Computing, Vienna, Austria (2017).

[33] R.W. Johnson, M.A. Dixon, D.R. Lee, Water relations of the tomato during fruit growth, Plant Cell Environment 15 (1992) 947-953.

[34] W.J. Lucas, A. Groover, R. Lichtenberger, K. Furuta, S.R. Yadav, Y. Helariutta, X-Q. He, H. Fukuda, J. Kang, S.M. Brady, J.W. Patrick, J. Sperry, A. Yoshida, A-F. Lopez-Millan, M.A. Grusak, P. Kachroo, The plant vascular system: evolution, development and functions, Journal of integrative plant biology 55 (2013) 294-388.

[35] R.M. Belda, L.C. Ho, Salinity effects on the network of vascular bundles during tomato fruit development, Journal of horticultural science 68 (1993) 557-564.

[36] E.J. Szymkowiak, E.E. Irish, Interactions between jointless and wild-type tomato tissues during development of the pedicel abscission zone and the inflorescence meristem, The Plant Cell 11 (1999) 159-175.

[37] J-L. Bonnemain, Anatomie et physiologie de l'appareil conducteur des Solanacées, Doctoral dissertation (1968).

[38] T. Nordey, M. Lechaudel, M. Génard, The decline in xylem flow to mango fruit at the end of its development is related to the appearance of embolism in the fruit pedicel, Functional Plant Biology 42 (2015) 668-675.

[39] M. Brüggenwirth, M. Knoche, Xylem conductance of sweet cherry pedicels, Trees 29 (2015)1851–1860.

[40] H. Van As, Intact plant MRI for the study of cell water relations, membrane permeability, cell-to-cell and long distance water transport, Journal of Experimental Botany 58 (2007) 743-756.

[41] S. Buy, S. Le Floch, N. Tang, R. Sidiboulenouar, M. Zanca, P. Canadas, E. Nativel, M. Cardoso, E. Alibert, G. Dupont, D. Ambard, C. Maurel, J-L. Verdeil, N. Bertin, C. Goze-Bac, C. Coillot, Flip-flop method: A new T1-weighted flow-MRI for plants studies, PLoS One 13 (2018) 1-14.

599 [42] J. Simon, M. Cardoso, E. Alibert, J-L. Verdeil, G. Vercambre, C. Goze-Bac, N. Bertin, Investigation and
600 integration of methods to better understand sap fluxes in tomato plant architecture, Acta Hortic. 1300 (2020)
601 55-62.
602 [43] P. Bussières, Water import in the young tomato fruit limited by pedicel resistance and calyx transpiration,
603 Functional Plant Biology 29 (2002) 631-641.
604 [44] J. Ripoll, L. Urban, M. Staudt, F. Lopez-Lauri, L.P. Bidel, N. Bertin, Water shortage and quality of fleshy
605 fruits - making the most of the unavoidable, Journal of Experimental Botany 65 (2014) 4097-4117.
606 [45] J-P. Renaudin, C. Deluche, C. Cheniclet, C. Chevalier, N. Frangne, Cell layer-specific patterns of cell
607 division and cell expansion during fruit set and fruit growth in tomato pericarp, Journal of experimental
608 botany 68 (2017) 1613-1623.
609 [46] C. Lovisolo, A. Schubert, Effects of water stress on vessel size and xylem hydraulic conductivity in Vitis
610 vinifera L., Journal of Experimental Botany 49 (1998) 693–700.
611 [47] J. Liu, S. Kang, W.J. Davies, R. Ding, Elevated [CO2] alleviates the impacts of water deficit on xylem
612 anatomy and hydraulic properties of maize stems, Plant, Cell Environment 43 (2019) 563-578.
613 [48] M. Mazzeo, B. Dichio, M.J. Clearwater, G. Montanaro, C. Xilioyannis, Hydraulic resistance of devel-
614 oping Actinidia fruit, Annals of Botany112 (2013) 197–205.
615 [49] E. Herremans, P. Verboven, M.L. Hertog, D. Cantre, M. van Dael, T. De Schryver, L.Van Hoorebeke,
616 B.M. Nicolaï, Spatial development of transport structures in apple (Malus × domestica Borkh.) fruit, Front
617 Plant Sci. 1 (2015) 679.
618 [50] P. Bussières, N. Bertin, C.E. Morris, C. Vigne, P. Orlando, C. Glaux, V. Sévenier, H. Floret, J. Bernadac,
619 S. Korownikoff, High external sucrose concentration inhibits the expansion of detached tomato fruits grown
620 in a novel semi-open device, In Vitro Cellular & Developmental Biology-Plant 47 (2011) 743-751.
621 [51] D. Constantinescu, G. Vercambre, M. Génard, Model-assisted analysis of the peach pedicel-fruit system
622 suggests regulation of sugar uptake and a water-saving strategy, J Exp Bot. 71 (2020) 3463-3474.
623

Table 1: Description of the eight genotype-dependent parameters used in the calibration step.

Parameter name	Description of the role
phiMax **[bar^{-1} h^{-1}]**	Maximum cell wall extensibility. Affects the cell expansion rate.
k **[h^{-1}]**	Parameter determining the decrease in plasticity during fruit aging. The higher the k value, the earlier the decrease in phiMax during fruit development
Lp **[m^4 MPa^{-1} s^{-1}]**	Conductivity of the composite membrane for water transport from phloem to fruit cell
Lx **[m^4 MPa-^{1} s^{-1}]**	Xylem conductivity for water transport within the fruit cell
nuM **[g sucrose gDM^{-1} h^{-1}]**	Maximum active sugar uptake rate. Part of the active sugar uptake calculation.
tstar **[h]**	Part of the active sugar uptake calculation. The higher the value of tstar, the later the decrease in active uptake during fruit development
tauA **[h]**	Part of the active sugar uptake calculation. The higher the value of tauA, the slower the decrease in active uptake rate during the growth stage
Lp1 **[m^3 MPa^{-1} s^{-1}]**	Phloem conductance for water transport in the pedicel
Lx1 **[m^3 MPa^{-1} s^{-1}]**	Xylem conductance for water transport in the pedicel

Figure captions

Figure 1: (A) Flower and pedicel of a WVA106 tomato plant. (B) Schematic representation of a tomato plant with red ripe and growing fruits on several trusses along the stem. FASGA-stained transverse histological sections of a WVA106 tomato showing (C) fruit pedicel (fruit side, AZf), (D) truss peduncle and (E) main stem. Red/pink zones indicate cells with lignified walls (secondary xylem and support fibers). Blue zones indicate cells with non-lignified cellulosic walls (phloem and parenchyma). Yellow lines correspond to the segmentation of the different tissue types. Segmentation was carried out using a plugin (PHIV_Tomate_toolset) developed ad-hoc on the Fiji open-source image processing package. This plugin allows measurement of the area of each segmented histological zone. For (C) and (E), section thickness: 60 µm. For (D), section thickness: 80 µm. For (C) and (D), scale bars: 1 mm. For (E), scale bar: 2 mm.

Figure 2: Transverse histological sections (thickness: 60 µm) stained by FASGA (scale bars: 1 mm) along the tomato pedicel of Heinz wild type (A) and Heinz Jointless (B) and relative proportions of tissues (C and D). (A, B) Left: fruit side of the pedicel (AZf); middle: actual (wild type) or theoretical (jointless: at the location of the pedicel curvature) abscission zone (AZ); right: stem side of the pedicel (AZs). (C, D) Each point represents an experimental measurement (3 to 8 pedicels per genotype and 1 to 8 microscopy samples per zone and pedicel). Error bars represent the standard deviation among fruits. Stars indicate significant differences between tissue proportions in the AZs and the AZf: *$p<0.05$, **$p<0.01$. Transverse sections.

Figure 3: Pedicel and fruit growth kinetics. (A) Pedicel diameter normalized bythe mean diameter value of each plant taken at the plateau as a function of fruit age normalized by age at maturity. (B) Fruit diameter normalized by the final diameter as a function of normalized fruit age (n=3 for each genotype). For (A) and (B) each point represents one plant/fruit at a given time, the different colors represent the different genotypes, and the black dashed line shows the time when pedicel growth reached a plateau. Measurements were carried out on reproductive plants bearing 7 to 10 fruiting trusses.

Figure 4: Fruit and pedicel traits according to genotype: (A) Final fruit fresh mass in g. (B) Final fruit dry matter content in g 100 g^{-1}. (C) Final pedicel diameter in mm. (D) Mean area proportions of the different tissues in the pedicel section. (E) Area of the vascular tissues in the pedicel section in μm^2. The Different shades represent the different tissues (see key). For (A), (B), (C), (D) and (E), genotypes are ranked from smaller to larger genotypes by fresh mass, from left to right. Three categories of fruit size are shown: small fruits (FM < 15g), large fruits (FM > 100g) and medium fruits (intermediate measurements). Each point represents a fruit. Measurements were carried out on reproductive plants bearing 7 to 10 fruiting trusses.

Figure 5: Influence of water deficit (WD) treatments on fruit and pedicel traits: (A) Final fruit fresh mass in g. (B) Final fruit dry matter content in g 100 g^{-1}. (C) Final pedicel diameter in mm. (D) Area of tissues in the pedicel section in μm^2. (E) Mean area proportions of tissues in the pedicel section. The different shades represent the different tissues (see key). Early WD occurred 15 days before truss anthesis, and late WD occurred 4 days after truss anthesis. Mild WD designates a 50 % reduction compared with the fully sufficient control irrigation regime and severe WD designates a 65 % reduction compared with the control. Each point represents a fruit. Stars indicate significant differences in the proportions of the different tissues between the designated treatment and the control treatment: *$p<0.05$, **$p<0.01$. Measurements were carried out on reproductive plants bearing 7 to 10 fruiting trusses.

Figure 6: Principal Component Analysis (PCA) of the virtual fruit parameters estimated for each genotype (active variables in red, see Table 1). Blue variables were projected as supplementary variables: fruit fresh mass (FM), fruit dry matter content (DMC), relative areas of the secondary xylem (secxyl_relval) and internal (intphl_relval) and external (extphl_relval) phloems, and absolute areas of the secondary xylem (secxyl_absval) and internal (intphl_absval) and external (extphl_absval) phloems. Variables are scaled to unit variance. Each genotype is represented by its barycenter. Cervil, WVA106 and Criollo are small fruit genotypes (FM<15g), Ferum, La0147 and Levovil are large fruit genotypes (FM>100g) and LA1420, Plovdiv and Stupicke are medium fruit genotypes (15 g < FM < 100 g). The third and fourth axes each accounted for 10 % of the variance, but did not discriminate well between genotypes (not shown).

A

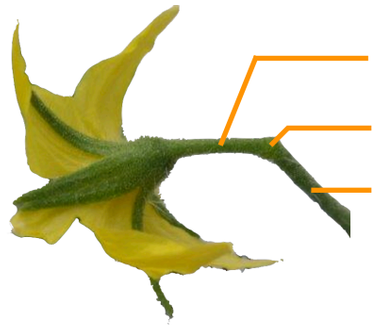

AZf
AZ
AZs

B

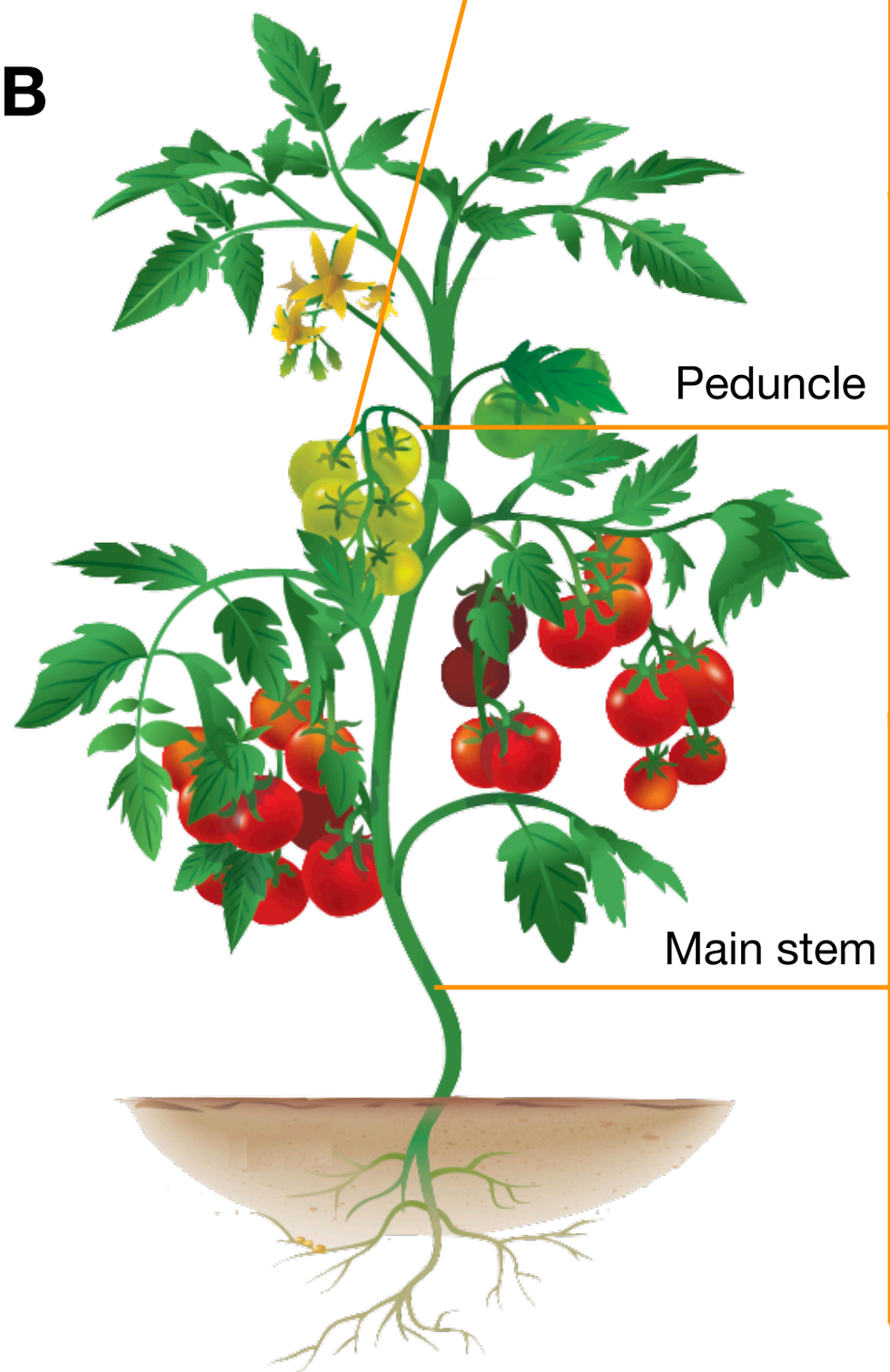

Pedicel
Peduncle
Main stem

C

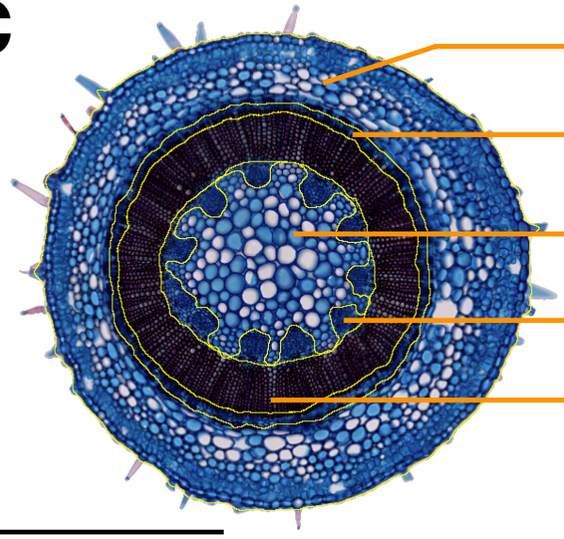

Cortex
External phloem
Pith
Internal phloem
Secondary xylem

D

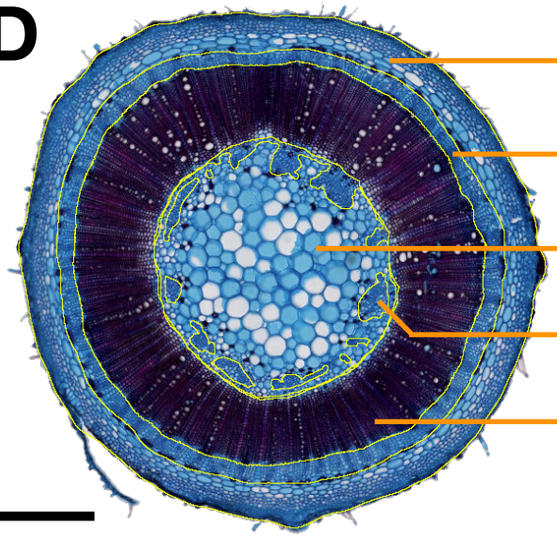

Cortex
External phloem
Pith
Internal phloem
Secondary xylem

E

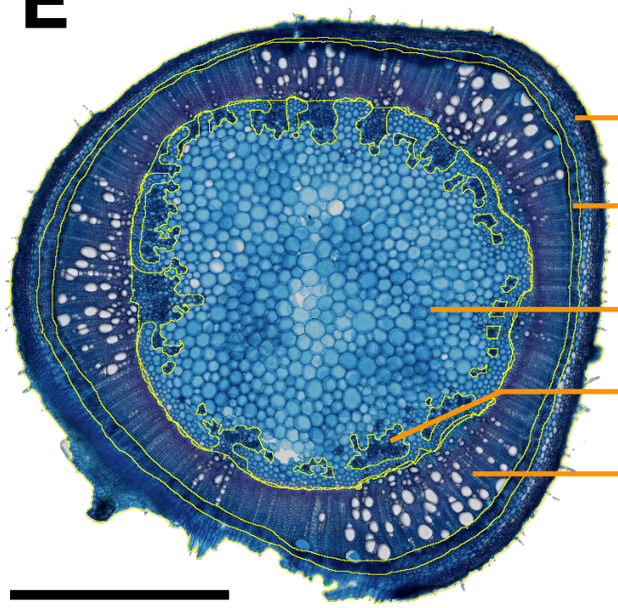

Cortex
External phloem
Pith
Internal phloem
Secondary xylem

Figure 1

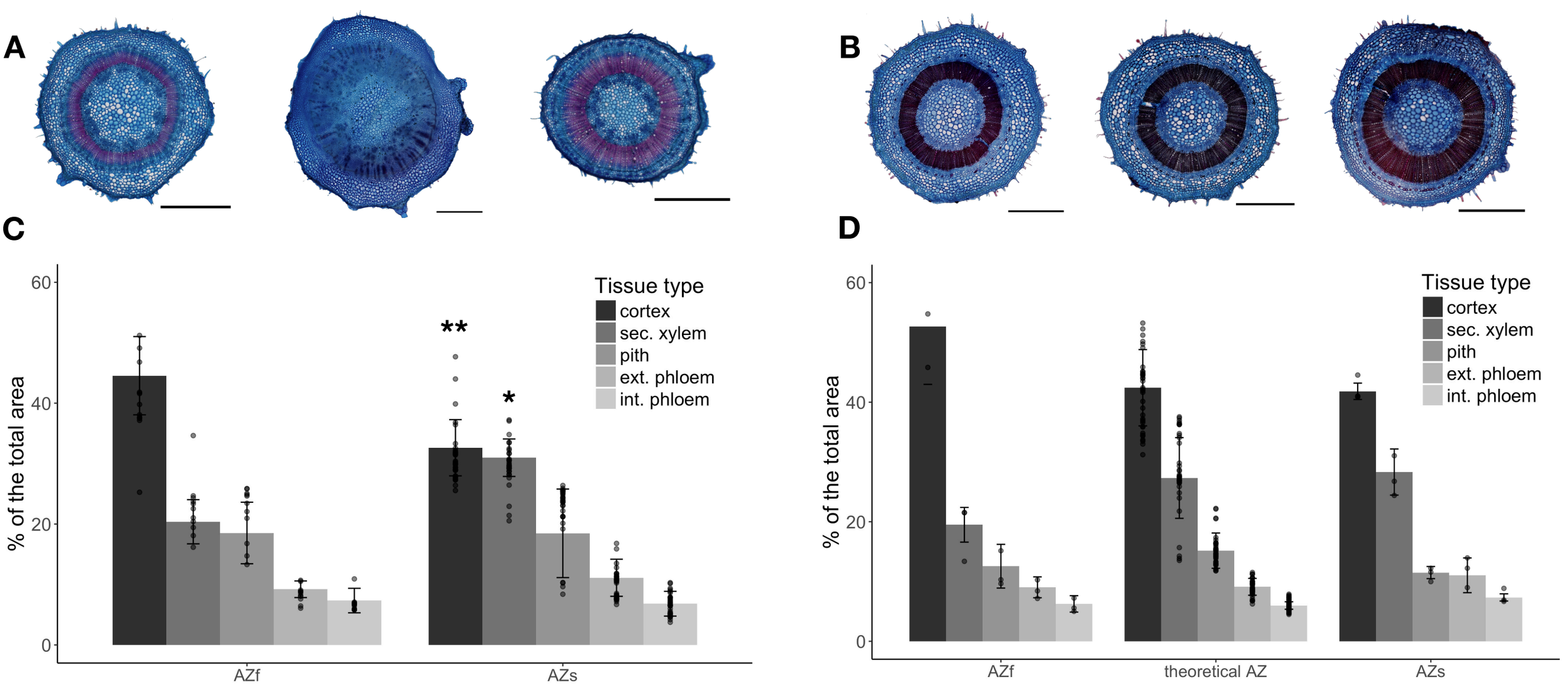
A
B
C
D
% of the total area
60
40
20
0
Tissue type
cortex
sec. xylem
pith
ext. phloem
int. phloem
**
*
AZf
AZs
theoretical AZ

Figure 2

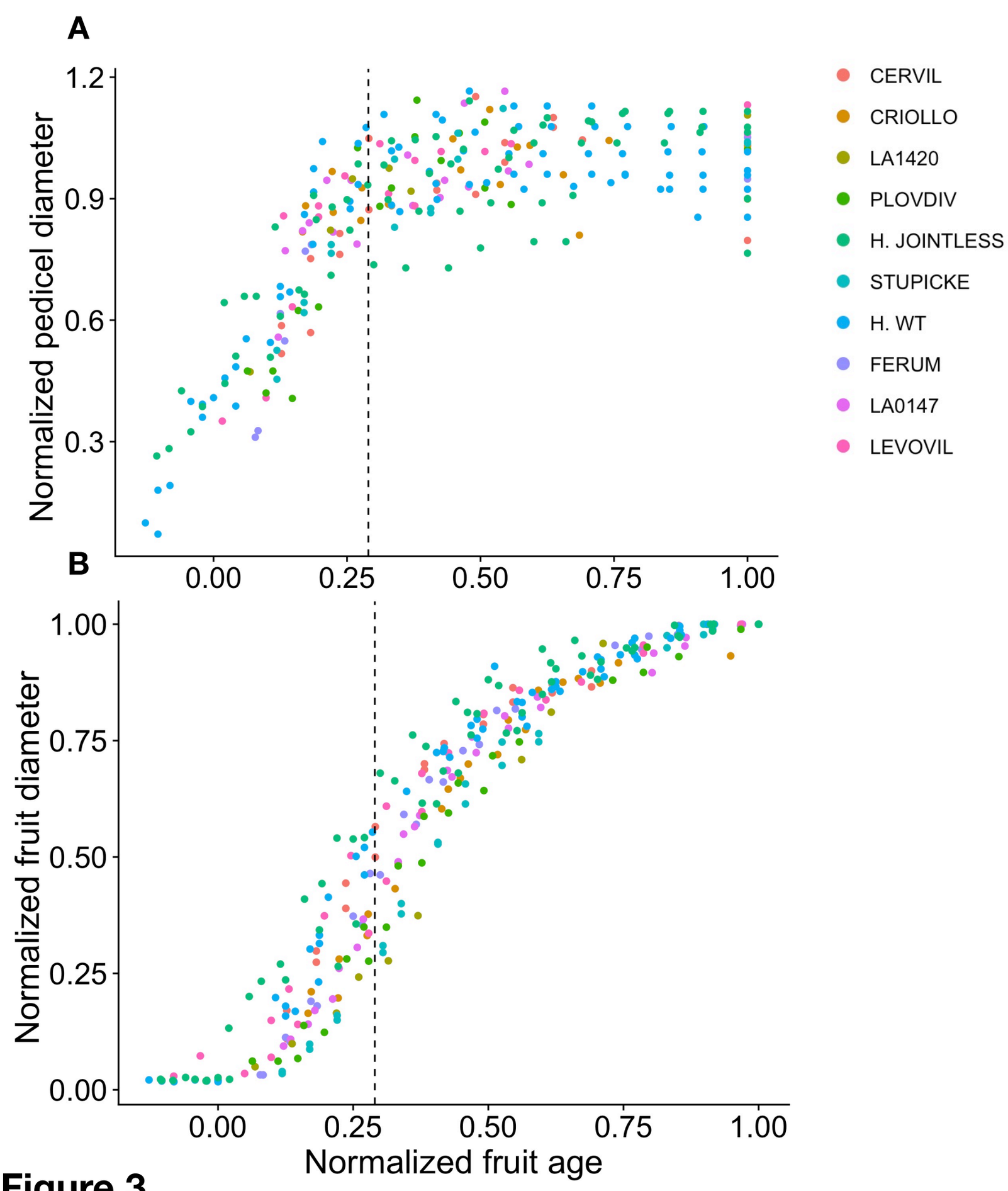
A
B
Normalized pedicel diameter
1.2
0.9
0.6
0.3
0.00
0.25
0.50
0.75
1.00
Normalized fruit diameter
Normalized fruit age
CERVIL
CRIOLLO
LA1420
PLOVDIV
H. JOINTLESS
STUPICKE
H. WT
FERUM
LA0147
LEVOVIL

Figure 3

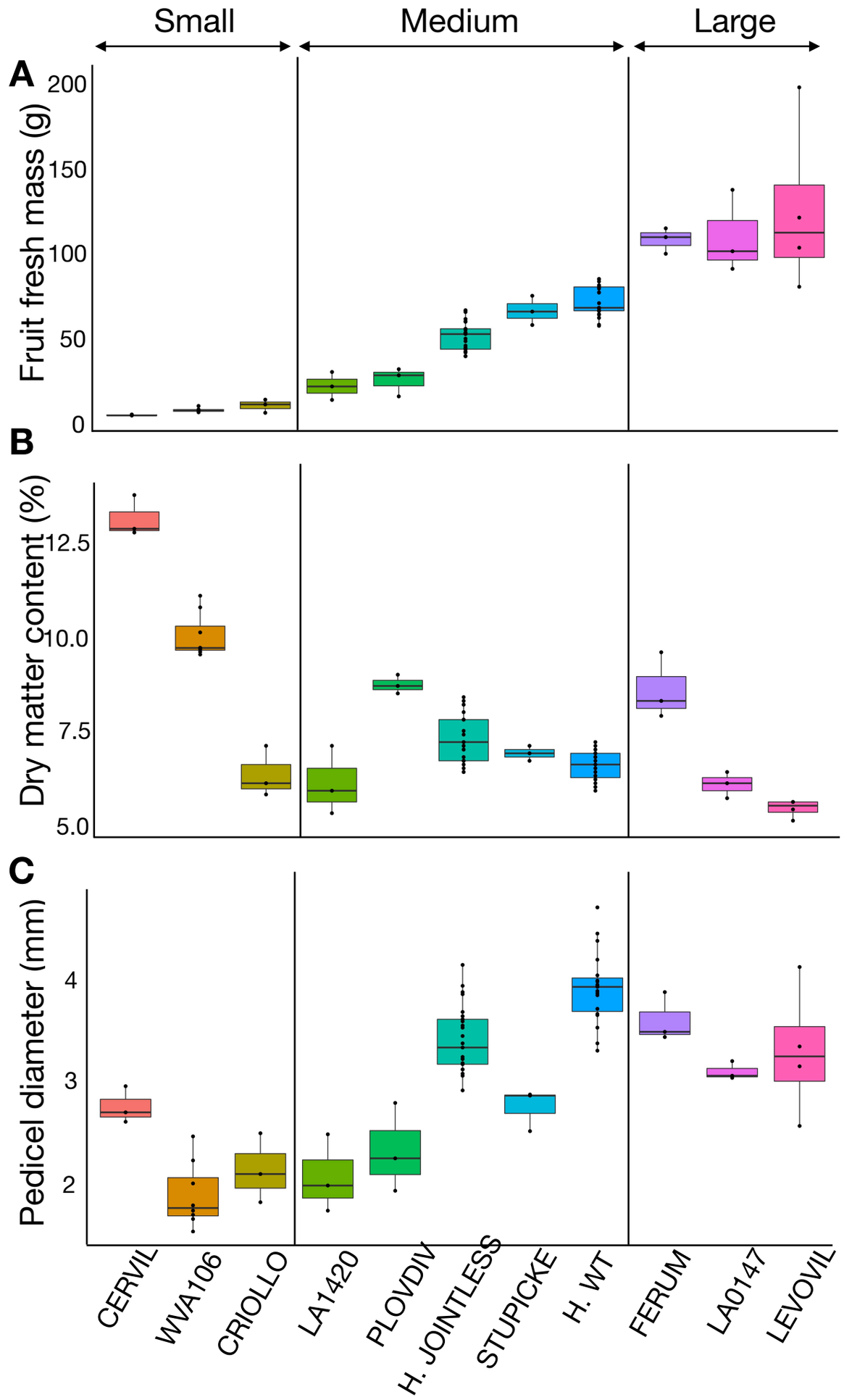
A
Small
Medium
Large
Fruit fresh mass (g)
0
50
100
150
200
B
Dry matter content (%)
5.0
7.5
10.0
12.5
C
Pedicel diameter (mm)
2
3
4
CERVIL
WVA106
CRIOLLO
LA1420
PLOVDIV
H. JOINTLESS
STUPICKE
H. WT
FERUM
LA0147
LEVOVIL

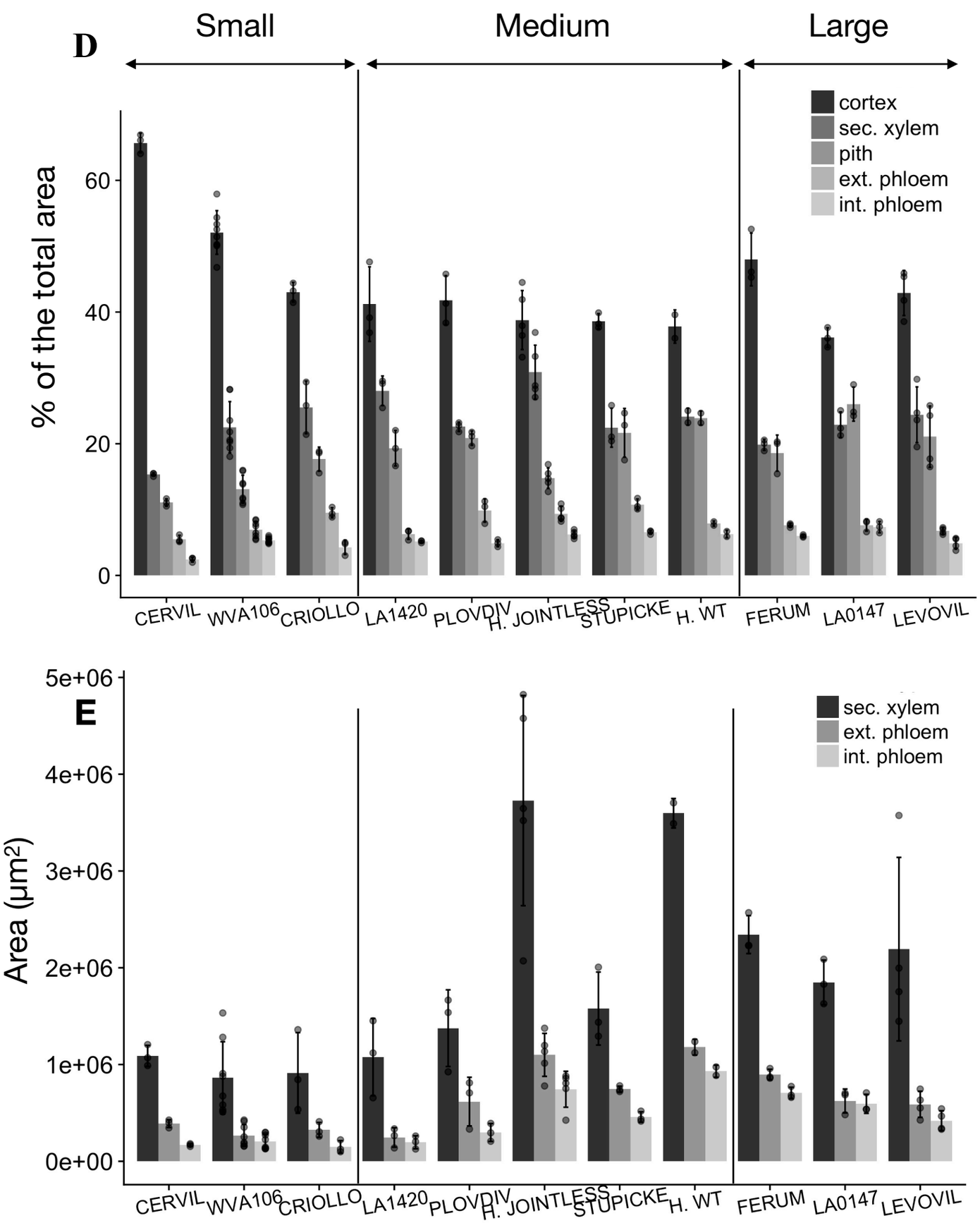
D
Small
Medium
Large
cortex
sec. xylem
pith
ext. phloem
int. phloem
% of the total area
0
20
40
60
CERVIL
WVA106
CRIOLLO
LA1420
PLOVDIV
H. JOINTLESS
STUPICKE
H. WT
FERUM
LA0147
LEVOVIL
E
sec. xylem
ext. phloem
int. phloem
Area (µm²)
0e+00
1e+06
2e+06
3e+06
4e+06
5e+06

Figure 4

Figure 5

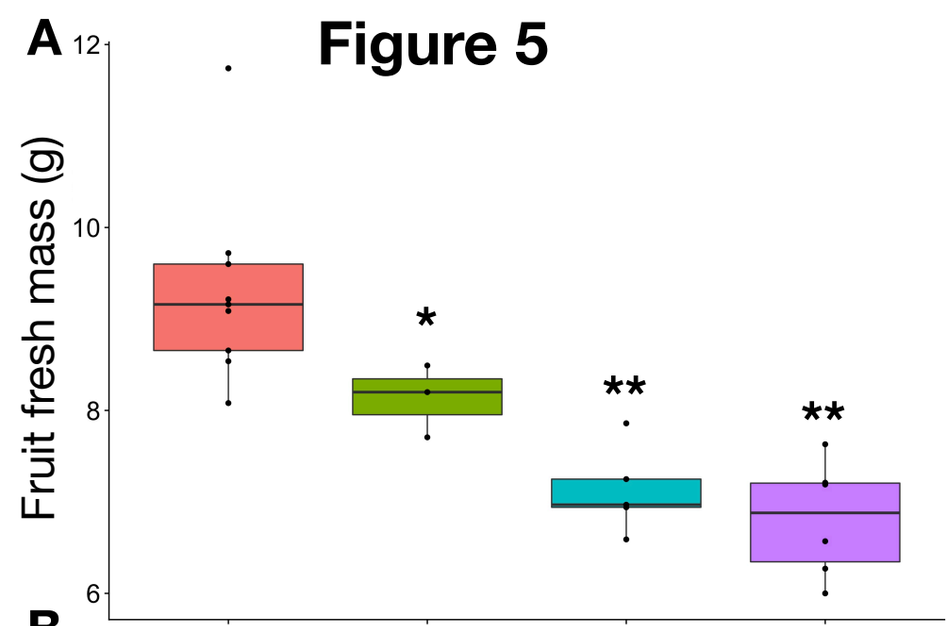
A
Fruit fresh mass (g)
12
10
8
6
*
**
**

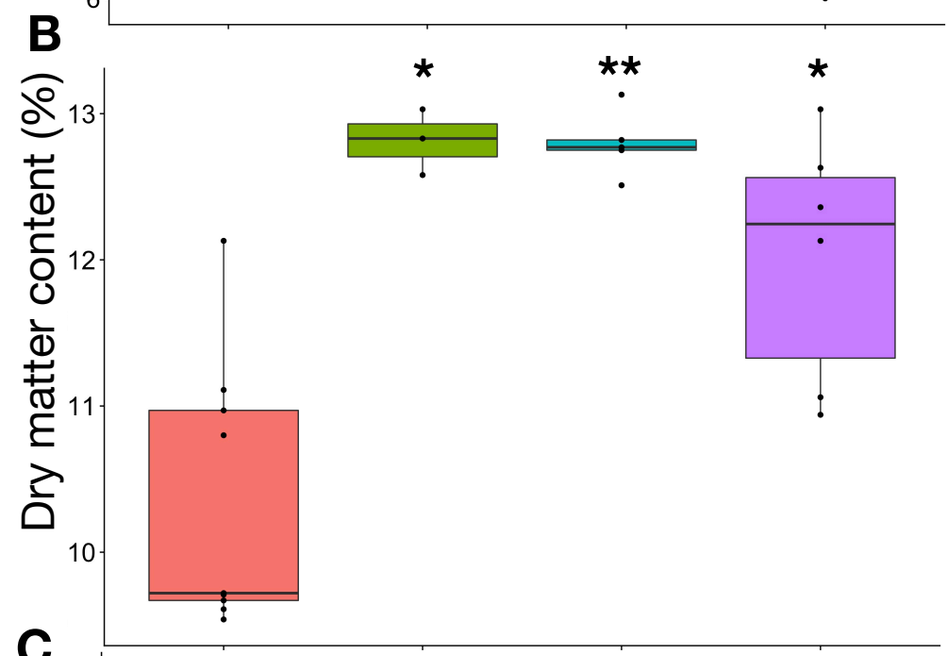
B
Dry matter content (%)
13
12
11
10
*
**
*

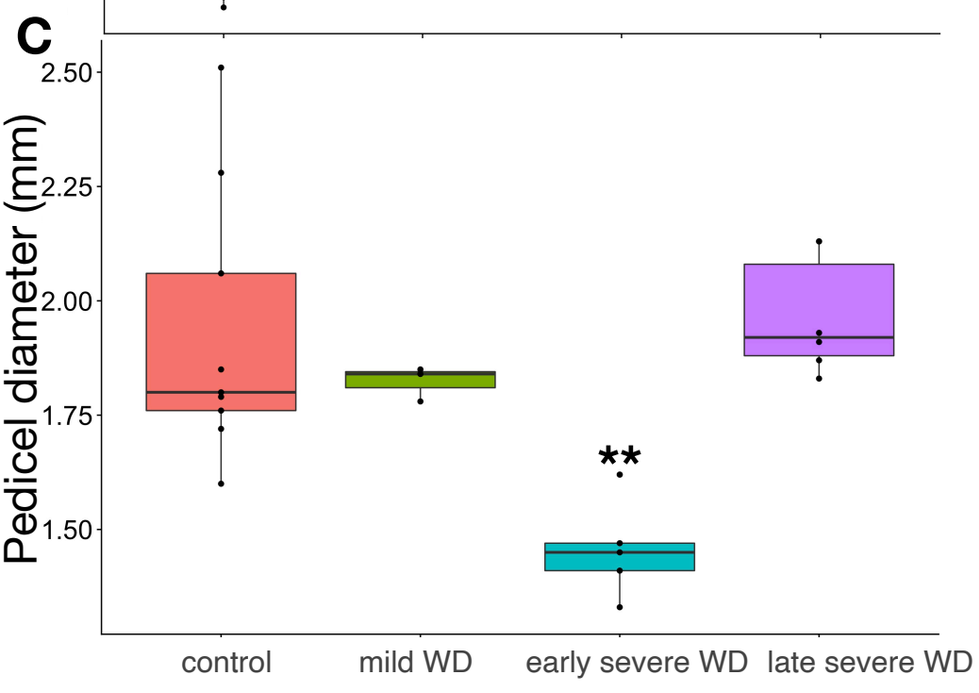
C
Pedicel diameter (mm)
2.50
2.25
2.00
1.75
1.50
**
control
mild WD
early severe WD
late severe WD

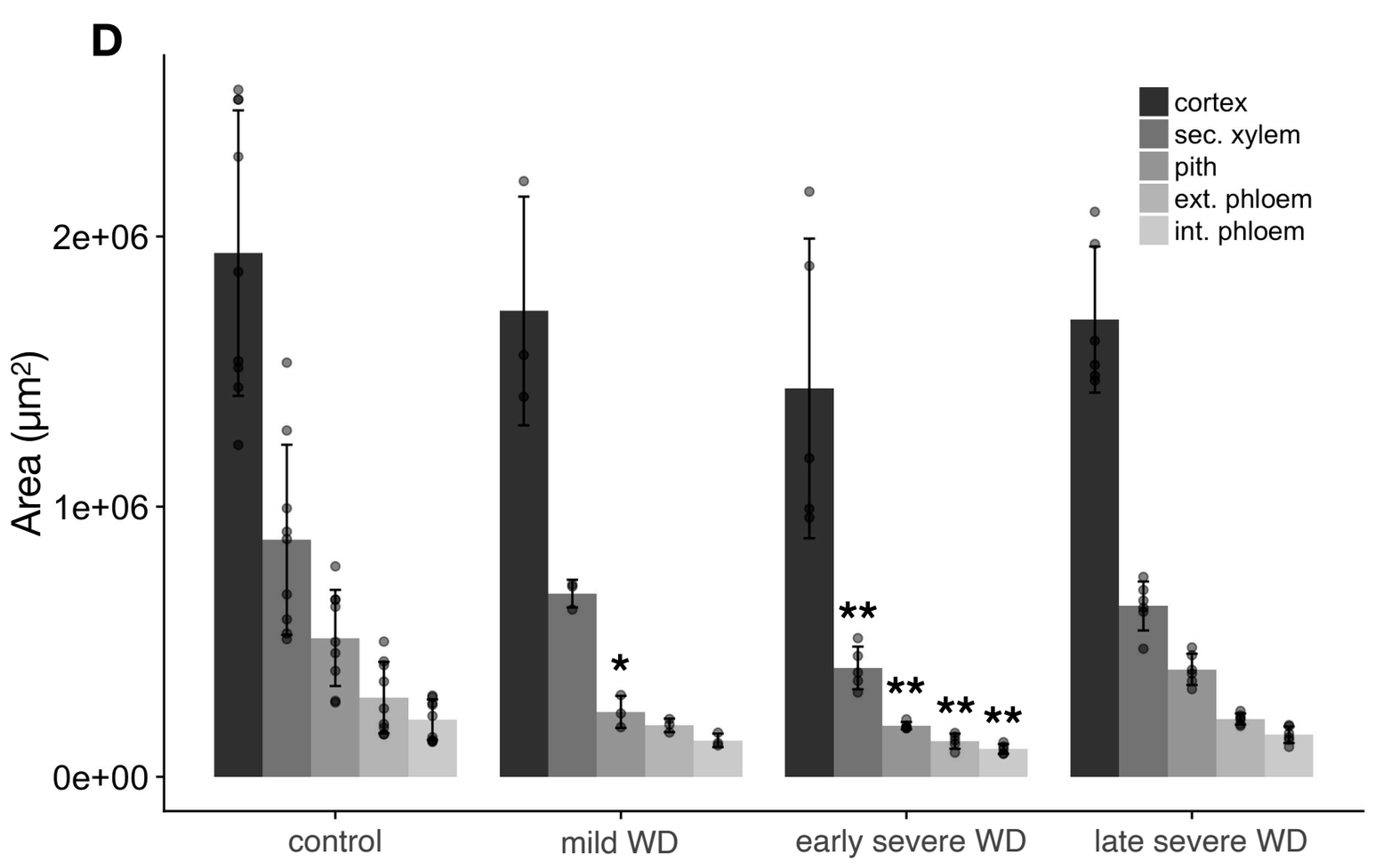
D
Area (µm²)
2e+06
1e+06
0e+00
cortex
sec. xylem
pith
ext. phloem
int. phloem
*
**
**
**
control
mild WD
early severe WD
late severe WD

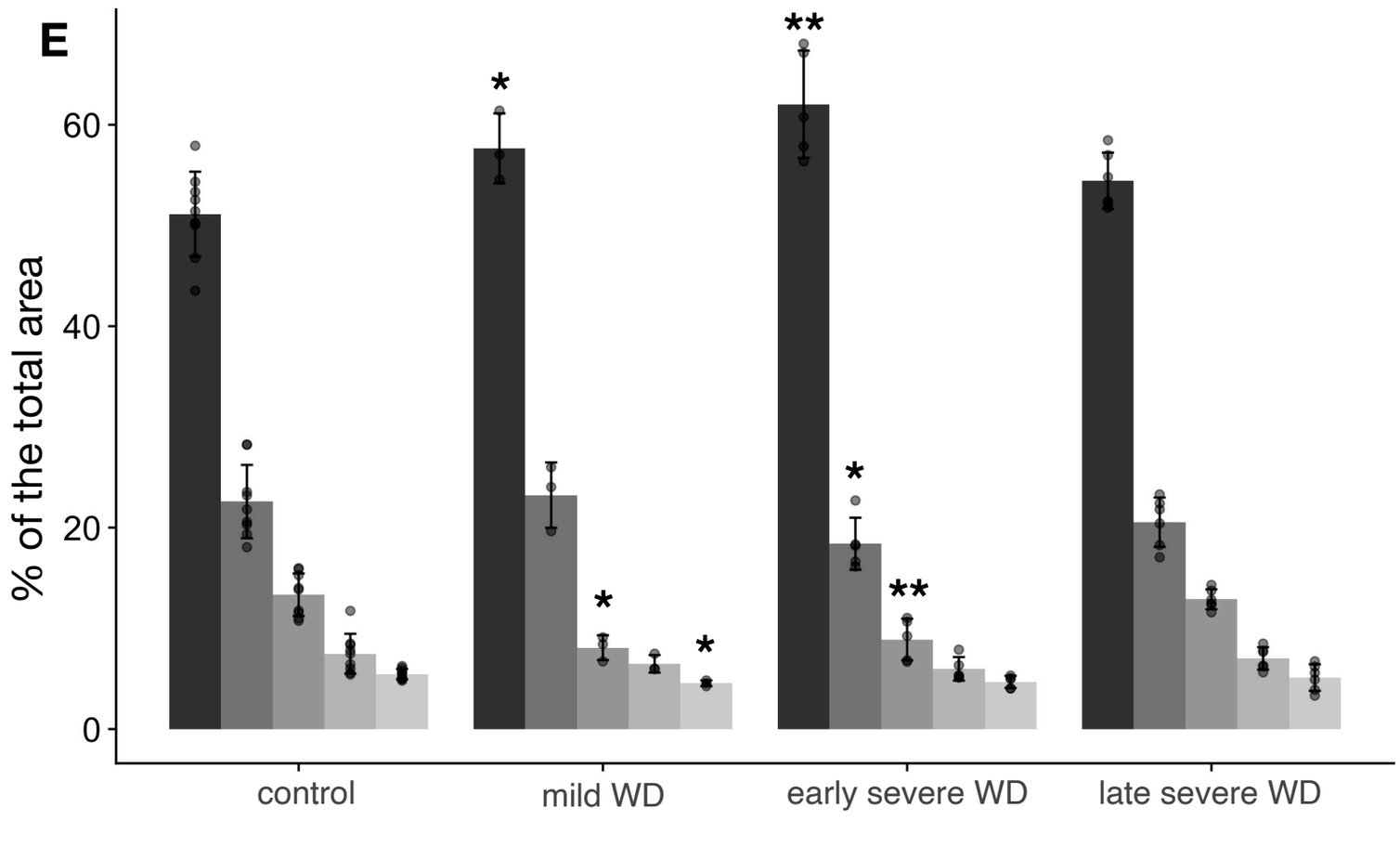
E
% of the total area
60
40
20
0
*
**
*
*
*
**
*
**
control
mild WD
early severe WD
late severe WD

Figure 6

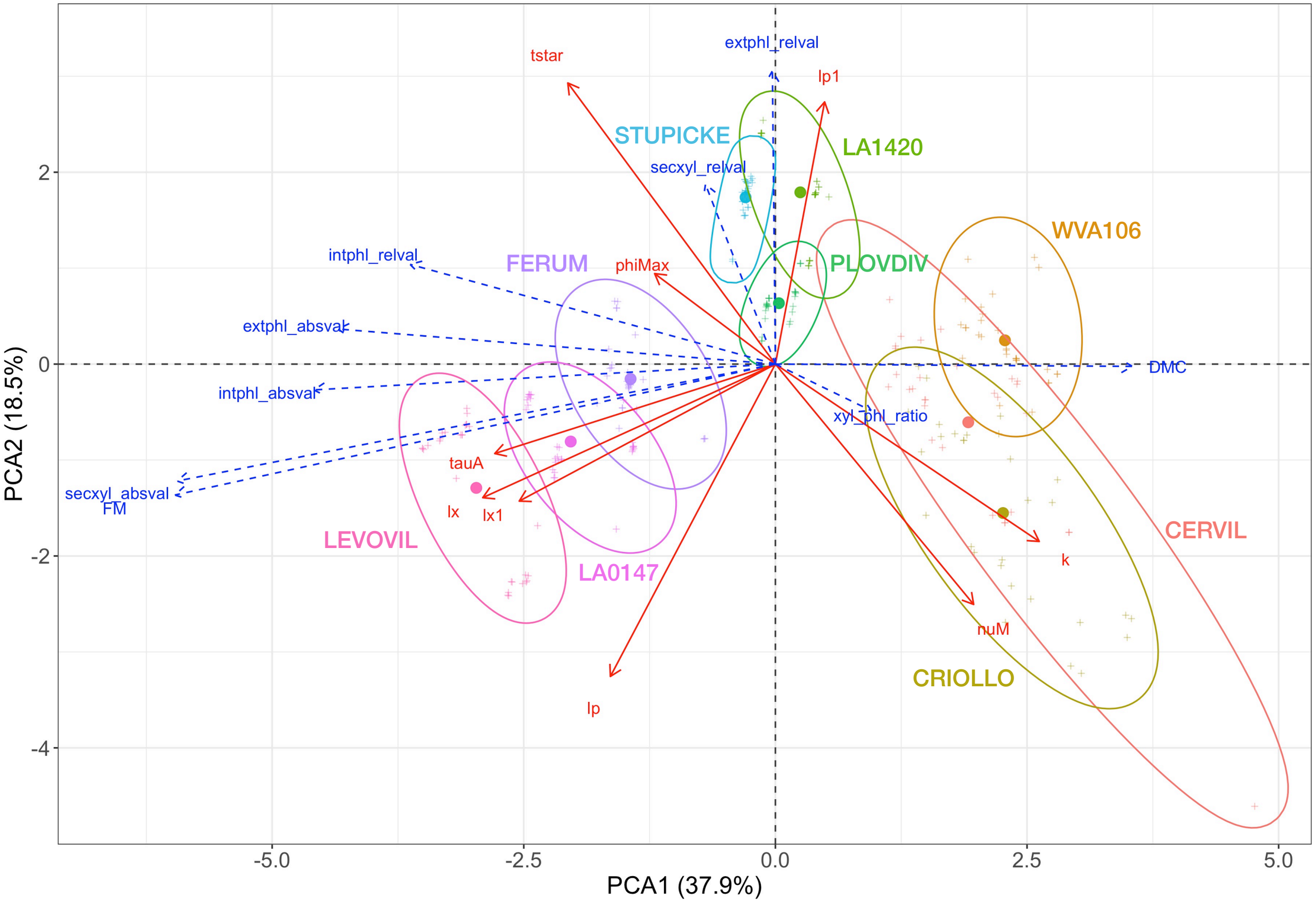
tstar
extphl_relval
lp1
STUPICKE
LA1420
secxyl_relval
WVA106
intphl_relval
FERUM
phiMax
PLOVDIV
extphl_absval
DMC
intphl_absval
xyl_phl_ratio
tauA
secxyl_absval
FM
lx
lx1
LEVOVIL
LA0147
CERVIL
k
nuM
CRIOLLO
lp
2
0
-2
-4
-5.0
-2.5
0.0
2.5
5.0
PCA2 (18.5%)
PCA1 (37.9%)